Laemmli, U. K. (1970) *Nature (London) 227*, 680–685.
Lowry, O. H., Rosebrough, N. J., Farr, A. L., & Randall, R. J. (1951) *J. Biol. Chem. 193*, 265–275.
Lux, S. E. (1979) *Nature (London) 281*, 426–429.
March, S. C., Parikh, I., & Cuatrecasas, P. (1974) *Anal. Biochem. 60*, 149–152.
Mescher, M. F., Jose, M. J. L., & Balk, S. P. (1981) *Nature (London)* (in press).
Parham, P. (1979) *J. Biol. Chem. 254*, 8709–8712.
Parham, P., Alpert, B. N., Orr, H. T., & Strominger, J. L. (1977) *J. Biol. Chem. 252*, 7555–7567.
Petty, H. R., Smith, L. M., Fearon, D. T., & McConnell, H. M. (1980) *Proc. Natl. Acad. Sci. U.S.A. 77*, 6587–6591.
Pober, J. S., Guild, B. C., & Strominger, J. L. (1978) *Proc. Natl. Acad. Sci. U.S.A. 75*, 6002–6006.
Robb, R. J. (1977) Ph.D. Thesis, Harvard University, Cambridge, MA.
Robb, R. J., Strominger, J. L., & Mann, D. L. (1976) *J. Biol. Chem. 251*, 5427–5428.
Robb, R. J., Terhorst, C., & Strominger, J. L. (1978) *J. Biol. Chem. 253*, 5319–5324.
Springer, T. A., & Strominger, J. L. (1976) *Proc. Natl. Acad. Sci. U.S.A. 73*, 2481–2485.
Springer, T. A., Strominger, J. L., & Mann, D. (1974) *Proc. Natl. Acad. Sci. U.S.A. 71*, 1539–1543.
Vesterberg, O., & Hansen, L. (1977) in *Electrofocusing and Isotachophoresis* (Radola, B. J., & Graesslin, D., Eds.) pp 123–133, de Gruyter, Elmsford, NY.

Interaction of Tropomyosin–Troponin with Actin Filaments†

Albrecht Wegner* and Terence P. Walsh

ABSTRACT: The assembly of actin filaments with tropomyosin–troponin was investigated by means of light scattering. Binding curves of tropomyosin–troponin [consisting of all three subunits (holotroponin)] and of tropomyosin–troponin-T–I to actin filaments were analyzed by separating the affinity of tropomyosin–troponin for actin filaments and the affinity for the end-to-end contact of tropomyosin molecules. Under the experimental conditions (42.4 °C, 300 mM KCl), tropomyosin–holotroponin in the absence of calcium and tropomyosin–troponin-T–I had similar affinities for actin filaments whereas tropomyosin–holotroponin in the presence of calcium was found to bind more weakly. Tropomyosin–holotroponin and tropomyosin–troponin-T–I bound about 200–300-fold more strongly to binding sites with adjacent tropomyosin–troponin units than to isolated sites on actin filaments. The equilibrium constant for isolated association with actin filaments was more than 2-fold higher for tropomyosin–holotroponin in the absence of calcium (15 400 M^{-1}) and tropomyosin–troponin-T–I (17 500 M^{-1}) than for tropomyosin–holotroponin in the presence of calcium (6600 M^{-1}). Binding curves of mixtures of tropomyosin–holotroponin in the presence of calcium and of tropomyosin–troponin-T–I were measured and analyzed on the basis of a model of cooperative binding of two types of large ligands to a one-dimensional homogeneous lattice. The results provided information on the strength of the end-to-end contacts of tropomyosin–troponin units in different positions on an actin filament. It was found that a tropomyosin–troponin unit binds adjacently to another unit in a different position on an actin filament about 2-fold more weakly than adjacent to a unit in the same position. With the aid of these results, it was possible to obtain information on the equilibrium distribution of tropomyosin–troponin in the two positions on actin filaments. Generation of a sequence of tropomyosin–troponin units in a different position on actin filaments was found to be 4-fold less favored than elongation of an existing sequence (cooperativity parameter $\sigma = {}^1/_4$). Shifting of tropomyosin–troponin on actin filaments appears to be accompanied by small free-energy changes in the various interactions of the components of actin–tropomyosin–troponin filaments and not to be an all-or-none reaction.

The regulatory role of the tropomyosin–troponin complex in muscle contraction was first described by Ebashi (1963), who showed that at low calcium concentrations the tropomyosin–troponin complex prevents the interaction of myosin with actin whereas at high calcium concentrations actin–tropomyosin–troponin filaments activate ATP hydrolysis by myosin. X-ray and electron microscopic investigations have provided evidence that tropomyosin is shifted from the periphery to the groove of actin filaments on binding of calcium to troponin (Huxley, 1972; Haselgrove, 1972; Parry & Squire, 1973; Wakabayashi et al., 1975; Seymour & O'Brien, 1980). The inhibition of myosin ATPase in the absence of calcium has been interpreted as a steric blocking of the myosin binding sites on actin filaments by tropomyosin (Huxley, 1972).

Troponin is composed of three nonidentical subunits (holotroponin), the molar ratios of which are still being discussed (Greaser & Gergely, 1971; Sperling et al., 1979). The three troponin subunits are designated troponin-T, the tropomyosin-binding subunit, troponin-I, which is necessary to inhibit the myosin ATPase, and troponin-C, which binds calcium. The tropomyosin–troponin-T–I complex inhibits the actomyosin ATPase independently of the calcium concentration (Greaser et al., 1972), and electron microscopic studies indicate that in actin–tropomyosin–troponin-T–I filaments the tropomyosin is located at the periphery of the actin filaments (Wakabayashi et al., 1975).

Myosin free of ATP binds to actin–tropomyosin–troponin filaments even in the absence of calcium (Bremel & Weber, 1972). Under these conditions, troponin has greater affinity

† From the University of Pennsylvania, School of Medicine, Department of Biochemistry and Biophysics, Philadelphia, Pennsylvania 19174. *Received January 27, 1981.* This study was supported by National Institutes of Health Grants HL 15835 and 15692.

* Address correspondence to this author at the Biozentrum, Abteilung Biophysikalische Chemie, CH-4056 Basel, Switzerland. A.W. received a fellowship from the Deutsche Forschungsgemeinschaft.

0006-2960/81/0420-5633$01.25/0

for calcium than in the absence of myosin, and bound nucleotide-free myosin molecules cause the filaments to activate the ATPase of myosin saturated with ATP (Bremel & Weber, 1972). Recently binding curves of myosin–subfragment-1–ADP to actin–tropomyosin–troponin filaments were analyzed (Hill et al., 1980) on the basis of a model that assumes that both in the presence and in the absence of calcium each actin subunit associated with tropomyosin–troponin can occur in one of two states which differ in the binding constants for subfragment-1 (Greene & Eisenberg, 1980). Furthermore, it was assumed that there are nearest neighbor interactions between tropomyosin–troponin units. Within the limits of this model, a positive cooperativity was found that favors binding of subfragment-1 to actin subunits covered by adjacent tropomyosin–troponin units over binding to actin subunits covered by separated tropomyosin–troponin units (Hill et al., 1980).

In this study the cooperativity of the shifting of tropomyosin–troponin on actin filaments was investigated by an analysis of the interactions of the various components.

Theory

In this section, a model will be derived on the basis of which information about cooperative conformational changes can be obtained from an analysis of binding to a homogeneous lattice of mixtures of two types of ligands. Each of the two types of ligands (tropomyosin–holotroponin and tropomyosin–troponin-T–I) is assumed to be bound to the actin filament in one of the two positions between which the conformational change occurs (shifting of tropomyosin from the groove to the periphery of actin filaments). Actin filaments are viewed as linear lattices of polarly arranged identical repeating subunits. Also, the tropomyosin–troponin complex is assumed to be polar, to bind in a fixed orientation with respect to the actin filament, and to cover seven consecutive subunits of an actin filament. The end-to-end contact formed by the termini of adjacently bound tropomyosin–troponin molecules is taken into account by introducing ligand–ligand interactions between nearest neighbors.

Each of the two types of ligands can bind to eight types of binding sites which differ in their binding constants (Figure 1). (I) Isolated binding sites: the ligands have no end-to-end contact with adjacent ligands (Figure 1, 1 and 2). (II) Singly contiguous binding sites: (1) the ligands have one end-to-end contact with a ligand of the same type (Figure 1, 3 and 6); (2) the ligands form an end-to-end contact on the left with a ligand of a different type (Figure 1, 4 and 7); (3) the ligands form an end-to-end contact on the right with a ligand of a different type (Figure 1, 5 and 8). (III) Doubly contiguous binding sites: (1) the ligands have two end-to-end contacts with ligands of the same type (Figure 1, 9 and 13); (2) the ligands have an end-to-end contact on the left with a ligand of the same type and on the right an end-to-end contact with a ligand of a different type (Figure 1, 10 and 14); (3) the ligands have an end-to-end contact on the left with a ligand of a different type and on the right an end-to-end contact with a ligand of the same type (Figure 1, 11 and 15); (4) the ligands form two end-to-end contacts with ligands of a different type (Figure 1, 12 and 16).

The equilibrium of the assembly of tropomyosin–troponin with bound calcium (ligand type a) and tropomyosin–troponin-T–I (ligand type b) with actin filaments may be described by six independent equilibrium constants, e.g., (1) K_a, equilibrium constant for the association of ligand a to an isolated binding site, (2) K_b, equilibrium constant for the association of ligand b to an isolated binding site, (3) J_{aa}, equilibrium constant for moving ligand a from an isolated binding site to a singly contiguous binding site with adjacent ligand a, (4) J_{ab}, equilibrium constant for moving ligand a from an isolated binding site to a singly contiguous binding site with adjacent ligand b on the right, (5) J_{ba}, equilibrium constant for moving ligand b from an isolated binding site to a singly contiguous binding site with adjacent ligand a on the right, and (6) J_{bb}, equilibrium constant for moving ligand b from an isolated binding site to a singly contiguous binding site with adjacent ligand b.

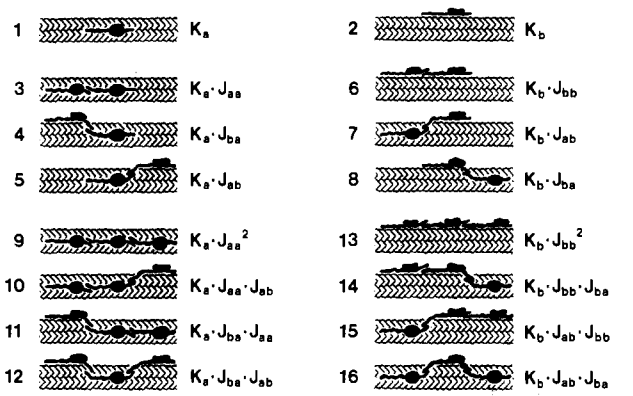

FIGURE 1: Kinds of binding sites. The tropomyosin–troponin unit in the center of the actin filaments is considered. (Left column) Binding sites for tropomyosin–troponin in the groove of actin filaments (tropomyosin–holotroponin in the presence of calcium). (Right column) Binding sites for tropomyosin–troponin on the periphery of actin filaments (tropomyosin–holotroponin in the absence of calcium or tropomyosin–troponin-T–I). The equilibrium constants are displayed on the right.

In Figure 1, the binding constants composed of the six independent equilibrium constants are displayed for the different types of binding sites. The composite binding constants can be derived by appropriate combinations of the simple reactions for which the six independent equilibrium constants have been defined.

The equilibrium of cooperative conformational changes of linear lattices is generally described by two equilibrium constants s and σ (Ising, 1925; Zimm & Bragg, 1959). s is the equilibrium constant for the elongation of a sequence of one state of the linear lattice, e.g., the shifting from the groove (a) to the peripheral position (b) of a tropomyosin–troponin unit adjacent to a unit situated in the peripheral position (b).

$$\text{aaaaabbb} \overset{s}{\rightleftharpoons} \text{aaaabbbb}$$

The equilibrium constant for the generation of a new sequence of one state is given by σs. For instance, the generation of a new sequence consists of shifting a medial groove unit (a) to the periphery (b).

$$\text{aaaaa} \overset{\sigma s}{\rightleftharpoons} \text{aabaa}$$

The cooperativity parameter σ describes the factor by which generation of a new sequence is less or more favored than elongation of an existing sequence. The parameter σ can also be taken as an equilibrium constant for the exchange of two adjacent ligands.

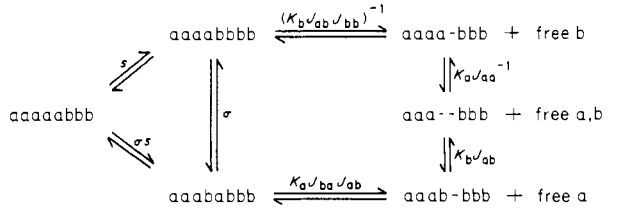

Therefore, the parameter σ can be related to the equilibrium constants of the end-to-end contacts by putting together the exchange reaction of dissociation of two ligands and consecutive association of these two ligands in inverted sequence. The cooperativity parameter σ is given by

$$\sigma = \frac{J_{ab}J_{ba}}{J_{aa}J_{bb}} \quad (1)$$

Binding equations which permit analysis of binding curves will be derived in the Appendix.

Experimental Procedures

(a) Preparation of the Proteins

Actin. Actin was prepared according to the method of Rees & Young (1967) with the alteration that the protein was purified by chromatography on a Bio-Gel P-150 column (2.5 × 90 cm) equilibrated with a buffer containing 500 μM ATP, 200 μM $CaCl_2$, 200 mg/L NaN_3, 1 mM dithiothreitol, and 5 mM triethanolamine–hydrochloric acid (pH 7.5) (Wegner & Engel, 1975).

Tropomyosin. The tropomyosin–troponin complex was extracted and purified by ammonium sulfate fractionation as described by Spudich & Watt (1971). Tropomyosin was separated from troponin by hydroxylapatite chromatography (Eisenberg & Kielley, 1974). By this procedure, tropomyosin was partially separated into its two multiple forms α,α- and α,β-tropomyosins. The first third of the fractions containing tropomyosin were used for the experiments. These fractions contained less than 5% β-tropomyosin chains or 10% α,β-tropomyosin as tested by electrophoresis (Wegner, 1980). Since the state of oxidation of cysteine-190 affects the assembly of the actin–tropomyosin complex (Walsh & Wegner, 1980), the protein was reduced by incubation with 20 mM dithiothreitol for 1 h at 40 °C (Lehrer, 1975).

Troponin. Holotroponin was extracted from rabbit skeletal muscle according to the method of Ebashi et al. (1971) with the modification that 0.5 mM phenylmethanesulfonyl fluoride and 0.01 mg of pepstatin and 0.1 mg of soybean trypsin inhibitor per mL (Sigma products) were included in the extraction solution. Following collection of the crude protein by ammonium sulfate fractionation (40–60%, pH 7.0), the solution was maintained at 0.1 mM EGTA until immediately before chromatography on hydroxylapatite and DEAE-cellulose (Whatman DE 52) by methods described by Clarke et al. (1976). The purified protein was stored as a lyophilized powder and showed no degradation as judged by $NaDodSO_4$ gel electrophoresis and ATPase assays.

Troponin-T–I. Tropomyosin-binding subunits and inhibitory subunits of troponin were isolated by DEAE-cellulose chromatography (Whatman DE 52) in the presence of 6 M urea (Margossian & Cohen, 1973; Horwitz et al., 1979). The starting material for these preparations was holotroponin or troponin-B prepared by the method of Wilkinson (1974). The complex of tropomyosin-binding and inhibitory subunits (troponin-T–I) was prepared by mixing the two subunits with an excess of the inhibitory subunit as described by Horwitz et al. (1979) with the alteration that the mixture was applied to a Bio-Gel P-150 column (2.5 × 35 cm) equilibrated with a buffer containing 500 mM KCl, 1 mM dithiothreitol, 200 mg/L NaN_3, and 5 mM triethanolamine hydrochloride (pH 7.5).

Tropomyosin–Troponin Complex. Following dialysis against 500 mM KCl, 1 mM dithiothreitol, 200 mg/L NaN_3, and 5 mM triethanolamine hydrochloride (pH 7.5), tropomyosin and holotroponin were mixed in a ratio of about 1:1.5. The concentration determination was based on extinction coefficients of 24 500 M^{-1} cm^{-1} for holotroponin (280 nm) (Margossian & Cohen, 1973). The tropomyosin–holotroponin complex was isolated from excess holotroponin by chromatography on Sepharose 6B. Ten milliliters of ~50 μM solution was applied to a 2.5 × 60 cm column equilibrated with a buffer containing 50 mM KCl, 1 mM dithiothreitol, 200 mg/L NaN_3, and 5 mM triethanolamine hydrochloride (pH 7.5). The composition of the fractions was analyzed by $NaDodSO_4$ gel electrophoresis. All fractions containing tropomyosin and holotroponin in a constant ratio were combined and used for the experiments.

An analogous preparation of the tropomyosin–troponin-T–I complex was not practicable since the troponin-T–I solutions obtained by the procedure described above were too diluted. The tropomyosin–troponin-T–I complex was formed by mixing equimolar amounts of tropomyosin and troponin-T–I. The concentrations were determined by using extinction coefficients of 24 500 M^{-1} cm^{-1} (276 nm) for tropomyosin and 27 800 M^{-1} cm^{-1} for troponin-T–I (280 nm) (Margossian & Cohen, 1973).

(b) Methods

ATPase assays were carried out with 5 μM S-1 and 2 μM actin. For assays of the calcium sensitivity, tropomyosin–troponin was mixed with actin at a molar ratio of 1:6.5 or 1:3 and dialyzed against 100 mM KCl, 1 mM $MgCl_2$, 1 mM dithiothreitol, and 10 mM imidazole at a protein concentration sufficient to produce a KCl concentration of 30 mM upon dilution into the assay medium. Actin–tropomyosin–troponin-T–I was similarly prepared except that the proteins were first mixed in 500 mM KCl and then reduced to 100 mM KCl by dialysis. All assays contained 1 mM free $MgCl_2$, 30 mM KCl, and either 200 μM $CaCl_2$ or 1 mM EGTA and were initiated by addition of Mg-ATP to give a 2 mM final concentration.

Light Scattering. All measurements were performed at 546 nm. The angular dependence of the light-scattering intensity was determined by using vertically polarized light. The photometer was calibrated by measuring the light-scattering intensity R_A of actin filaments of the same concentration as that present in the actin–tropomyosin–troponin samples. The light intensity of the cells containing pure buffer was subtracted from the total scattering intensity. The light-scattering intensity $R(\vartheta)$ of long polydisperse rodlike protein aggregates such as actin filaments or actin filaments completely covered with tropomyosin–troponin has been shown to be given by (Casassa, 1955)

$$R_A(\vartheta) = K\left[\frac{\lambda}{4 \sin (\vartheta/2)}\right]\left(\frac{M_A}{L_A}\right)C_A \quad (2)$$

where ϑ is the observation angle, K is an optical constant, C_A is the weight concentration of the filaments, λ is the wavelength of light in the solvent, M_A is the molecular weight of a filament subunit, and L_A is the length per filament subunit. Equation 2 has been derived for long rodlike particles the length of which exceeds $\lambda/[4\pi \sin (\vartheta/2)]$ and the diameter of which is smaller than $\lambda/[4\pi \sin (\vartheta/2)]$.

Equation 2 can be modified for rodlike filaments with an inhomogeneous mass per length distribution such as actin filaments partially covered with tropomyosin–troponin (Wegner, 1979):

$$R_T(\vartheta) = K\left[\frac{\lambda}{4 \sin (\vartheta/2)}\right]\left(\frac{M_A}{L_A}\right)\left[\frac{(C_A + C_T)^2}{C_A}\right] \quad (3)$$

When eq 2 and 3 are combined, a formula is obtained that allows the weight concentration of bound tropomyosin–troponin C_T to be calculated from the ratio of the scattering intensity of actin–tropomyosin–troponin filaments R_T to that of actin filaments R_A and the weight concentration of actin filaments C_A.

$$\frac{R_T}{R_A} = \frac{(C_A + C_T)^2}{C_A^2} \quad (4)$$

(For a test of the applicability of eq 2–4 to the actin–tropomyosin–troponin system, see Results.)

Preparation of Samples. All solutions were centrifuged for 30 min at 100000*g* to remove dust. The tropomyosin–troponin complex was formed by mixing 1 volume of a calcium-containing buffer with 6 volumes of a tropomyosin–troponin solution and 3 volumes of a monomeric actin solution. The calcium buffer was composed of 1.4 mM $CaCl_2$, 4 mM $MgCl_2$, 3.5 mM ATP, 1 mM dithiothreitol, 200 mg/L NaN_3, and 5 mM triethanolamine hydrochloride (pH 7.5). Tropomyosin–troponin solutions contained 500 mM KCl, 1 mM dithiothreitol, 200 mg/L NaN_3, and 5 mM triethanolamine hydrochloride (pH 7.5). Actin solutions contained 200 μM $CaCl_2$, 500 μM ATP, 1 mM dithiothreitol, 200 mg/L NaN_3, and 5 mM triethanolamine hydrochloride (pH 7.5). Hence, the composition of the mixed buffers was 200 μM $CaCl_2$, 400 μM $MgCl_2$, and 5 mM triethanolamine hydrochloride (pH 7.5). For measurements in the absence of calcium, 4 mM EGTA was included in the calcium buffer instead of calcium. The three components were combined in light-scattering cells (1 × 1 × 4 cm). The mixtures were warmed to 25 °C to avoid later formation of air bubbles. The light-scattering intensity of the samples reached a constant value after 15 h at room temperature, indicating that this time was necessary to form actin–tropomyosin–troponin filaments from monomeric actin, tropomyosin, and troponin.

Determination of Protein Concentrations. Actin concentration was determined photometrically at 290 nm by using an extinction coefficient of 24900 M^{-1} cm^{-1} (Wegner, 1976). The molecular weight was assumed to be 42300 (Elzinga et al., 1973). Photometric measurements of tropomyosin–troponin concentrations were not sufficiently accurate because of the unknown contribution of oxidized dithiothreitol to the absorption. Therefore the tropomyosin–troponin concentration equivalent to actin was determined by titration of actin filaments (see Results; Figure 3). For calculation of the weight concentrations, the molecular weights of tropomyosin–holotroponin and tropomyosin–troponin-T–I were assumed to be 135000 and 117000, respectively (Stone et al., 1975; Pearlstone et al., 1976; Wilkinson & Grand, 1975; Collins et al., 1977).

Electrophoresis. Polyacrylamide–$NaDodSO_4$ electrophoresis was performed according to the method of Laemmli (1970). Electrophoresis was used for the semiquantitative determination of protein concentrations and for tests of the purity and stability of proteins. For the determination of the concentration of monomeric actin and of tropomyosin–troponin not bound to actin filaments, the samples were centrifuged at 100000*g* for 1 h. The supernatants were applied to gel columns (6 × 70 mm). The gels were stained for 10 h with Fast Green (1 g of dye in 500 mL of methanol, 50 mL of acetic acid, and 450 mL of water) and destained in a methanol–acetic acid–water mixture (10:1:9). The gels were scanned photometrically at 625 nm. The areas below the tracings were calibrated by a series of gels to which solutions of known actin, tropomyosin, or troponin concentrations were applied.

Results and Discussion

(*a*) *Test of the Protein Preparations.* The tropomyosin–troponin preparations were tested by ATPase assays and light scattering. Holotroponin displayed 70–75% inhibition when tropomyosin–troponin was present in a 10% excess over actin. Increasing the ratio of tropomyosin–troponin to actin to 1:3 resulted in 89–92% inhibition. Tropomyosin–troponin-T–I showed no effect of calcium on the acto-S-1 ATPase. When tropomyosin–holotroponin or tropomyosin–troponin-T–I was bound to actin filaments, the maximum increase in light-scattering intensity was 1.95–2.05- or 1.95-fold, respectively, compared to the scattering intensity of actin filaments (Figure 3). On the basis of the increase in light-scattering intensity (see eq 4), the molecular weights of tropomyosin–holotroponin and of tropomyosin–troponin-T–I can be calculated to be 123000 or 117000, respectively, when a molecular weight of 42300 for actin monomers and a 7:1 molar ratio of the actin–tropomyosin–troponin complex is assumed. The molecular weights calculated on the basis of the amino acid sequences are 135000 and 117000. Mixing of troponin-T–I with tropomyosin in a higher ratio than that described above did not cause any further increase in the light-scattering intensity, indicating that tropomyosin was saturated with troponin-T–I and that excess troponin-T–I did not bind to actin filaments.

(*b*) *Light Scattering.* So that the applicability of eq 2–4 to the actin–tropomyosin–troponin system could be tested, the angular dependence of the light-scattering intensities of actin filaments and of actin filaments covered with tropomyosin–troponin was measured. Figure 2 shows that the reciprocal of the scattering intensity is nearly proportional to the sine of the half-observation angle (eq 2 and 3) and that the ratio of the scattering intensities R_T/R_A is almost independent of the observation angle (eq 4). Furthermore the 90° light-scattering intensities of actin filaments covered with various amounts of tropomyosin–troponin were measured; the square root of the scattering intensity, normalized by the scattering intensity of pure actin filaments, increases almost linearly with the tropomyosin–troponin concentration (eq 4) (Figure 3). At higher tropomyosin–troponin concentrations, the scattering intensity reaches a constant value. At these concentrations, actin filaments were saturated with tropomyosin–troponin, and unbound tropomyosin–troponin was observed by electrophoresis of the supernatants of centrifuged samples (Figure 3).

(*c*) *Experimental Conditions.* The actin–tropomyosin–troponin mixtures contained 300 mM KCl, 400 μM $MgCl_2$ and 200 μM $CaCl_2$. At lower potassium concentrations, tropomyosin–troponin was found to bind to actin filaments so strongly that the binding curves had to be measured at actin and tropomyosin–troponin concentrations that are too low for determination by light scattering. At higher concentrations, potassium chloride retarded the formation of actin–tropomyosin–troponin filaments to such an extent that assembly of the filaments was not completed within 1 day. Also, higher concentrations of calcium chloride appeared to retard the formation of actin–tropomyosin–troponin filaments from monomeric actin, tropomyosin, and troponin. Above 50 μM, variations in the calcium concentration did not influence the affinity of tropomyosin–troponin for actin filaments.

At the low actin concentrations (7 μM) and the high salt concentrations used in these experiments, corrections must be applied for monomeric actin coexisting with actin filaments [critical monomer concentration (Oosawa & Kasai, 1962)]. The critical concentration of pure actin was determined by extrapolating a plot of the light-scattering intensity vs. the total actin concentration to zero scattering intensity and by

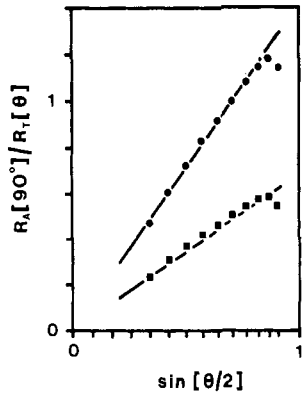

FIGURE 2: Plot of the sine of the half-observation angle vs. the reciprocal light-scattering intensity normalized by the 90° scattering intensity of pure actin. (●) Actin; (□) actin filaments completely saturated with tropomyosin–holotroponin.

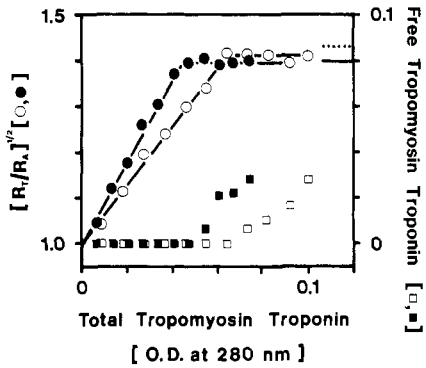

FIGURE 3: Total tropomyosin–troponin concentration expressed by the absorption at 280 nm vs. the square root of the light-scattering intensity normalized by the scattering intensity of pure actin filaments: (○) tropomyosin–holotroponin; (●) tropomyosin–troponin-T–I. Total tropomyosin–troponin concentration vs. the free tropomyosin–troponin concentration determined in the supernatant of centrifuged solutions: (□) tropomyosin–holotroponin; (■) tropomyosin–troponin-T–I. The scattering intensity calculated on the basis of a 1:7 stoichiometry and of the molecular weights of the proteins are given on the right; (···) tropomyosin–holotroponin and (—) tropomyosin–troponin-T–I.

measuring the actin concentration in the supernatant of centrifuged solutions. The critical concentration of pure actin was found to be 0.5 or 0.4 μM, respectively (Figure 4). The critical monomer concentration measured in the presence of different tropomyosin–troponin concentrations was also in the range of 0.4 μM, tending to be lower with increasing concentrations of tropomyosin–troponin (Figure 4). The concentration of actin filament subunits was obtained by subtraction of 0.4 μM from the total actin concentration.

(d) Binding Curves of Tropomyosin–Holotroponin or Tropomyosin–Troponin-T–I to Actin Filaments. The samples contained tropomyosin–holotroponin or tropomyosin–troponin-T–I in the concentration range from 0.1 to 1.5 μM, with the total actin concentration kept constant at 7 μM. The binding curves were measured in the presence and absence of calcium. Near 40 °C, the scattering intensity of the actin–tropomyosin–troponin solutions depended strongly on the temperature whereas the scattering intensity of pure actin filaments was constant from 15 to 45 °C. The changes in the light-scattering intensity of actin–tropomyosin–troponin solutions were reversible with temperature changes (Figure 5). A 10-min incubation of the actin–tropomyosin–troponin filaments in a constant temperature-controlled copper block was sufficient to reach similar light-scattering intensities on heating or cooling to the same temperature, indicating that within this time the association of tropomyosin–troponin with actin filaments reaches equilibrium. Longer incubation above room temperature was avoided because of the possible instability of troponin. Following the measurements, electrophoresis was

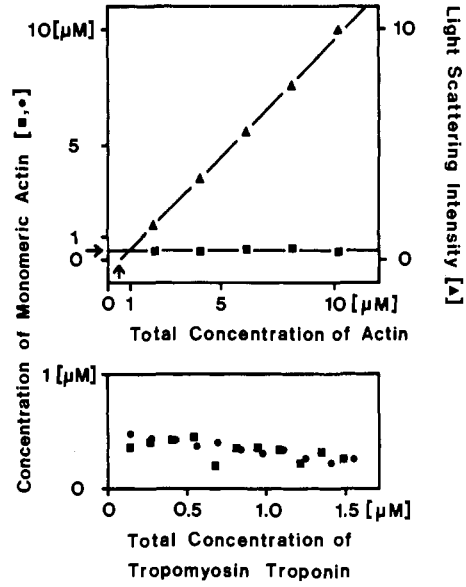

FIGURE 4: Determination of the critical monomer concentration of actin. (Top) Actin in the absence of tropomyosin–troponin. (▲) Light-scattering intensity normalized by the scattering intensity of 1 μM actin filament subunits vs. total actin concentration. Extrapolation to zero light-scattering intensity gives the critical monomer concentration indicated by an arrow (~0.5 μM). (■) Monomeric actin determined in the supernatant of centrifuged solutions with various total actin concentrations. The critical monomer concentration is indicated by an arrow on the left (~0.4 μM). (Bottom) Critical monomer concentration of actin in the presence of different tropomyosin–troponin concentrations. Total actin concentration, 7 μM. Monomeric actin was determined in the supernatant of centrifuged solutions. (■) Tropomyosin–holotroponin in the presence of calcium; (●) Tropomyosin–troponin-T–I.

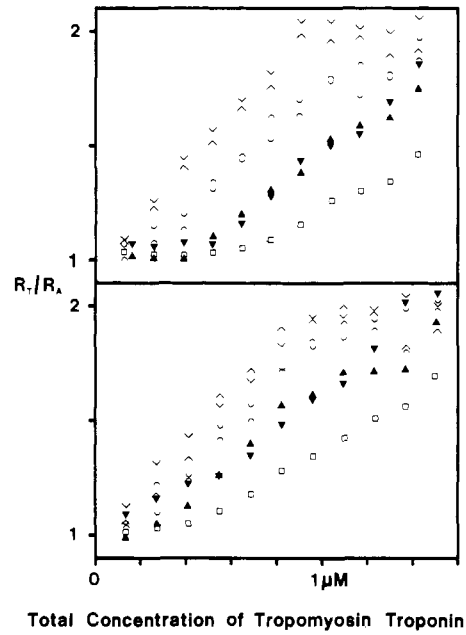

FIGURE 5: Temperature dependence of the normalized light-scattering intensity of actin–tropomyosin–troponin mixtures at various concentrations of tropomyosin–troponin. The concentration of polymeric actin was 6.6 μM. (Top) Tropomyosin–holotroponin; (bottom) tropomyosin–troponin-T–I. (^) 15 °C; (^) 41.1 °C after heating from 15 °C; (▲) 42.4 °C after heating from 41.1 °C; (□) 43.7 °C after heating from 42.4 °C; (▼) 42.4 °C after cooling from 43.7 °C; (∪) 41.1 °C after cooling from 42.4 °C; (∨) 15 °C after cooling from 41.1 °C.

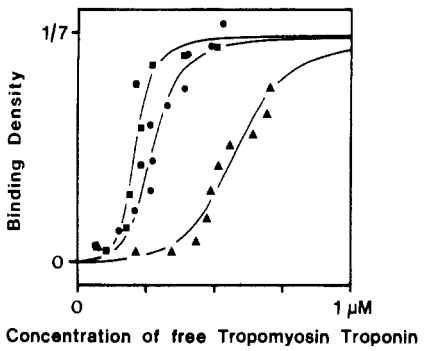

FIGURE 6: Binding curves of tropomyosin–troponin to actin filaments at 42.4 °C. The concentration of polymeric actin was 6.6 μM. (■) Tropomyosin–holotroponin in the absence of calcium; (▲) tropomyosin–holotroponin in the presence of calcium; (●) tropomyosin–troponin-T–I (this curve was measured in the presence of calcium; replacing calcium by EGTA had no effect on the binding curve).

used to examine samples for hydrolyzed troponin. If proteolysis was observed, the measurements were disregarded. Usually the samples containing actin in a stoichiometric excess over tropomyosin–troponin were found to be intact whereas slight proteolysis was repeatedly observed in solutions with a stoichiometric excess of tropomyosin–troponin.

From the light-scattering intensity and the total concentrations of actin and tropomyosin–troponin, plots of the binding density vs. the free tropomyosin–troponin concentration were calculated with the aid of eq 4 (Figure 6). The binding curves are sigmoidal, indicating cooperative association of tropomyosin–troponin with actin filaments. By analogy with the actin–tropomyosin system (Wegner, 1979), the cooperativity of assembly can be explained in terms of end-to-end contacts that are formed by the tropomyosin–troponin units when they are bound along the actin filament. A reaction scheme is obtained by reducing the number of types of ligands shown in Figure 1 to one. Tropomyosin–troponin can bind to three kinds of binding sites, namely isolated sites (Figure 1, filament 1 or 2), singly contiguous sites (Figure 1, filament 3 or 6), and doubly contiguous sites (Figure 1, filament 9 or 13). This equilibrium is described by two pairs of equilibrium constants K_a, J_{aa} and K_b, and J_{bb}. The theoretical aspects of the interaction of one type of large ligands with a lattice have been treated by McGhee & von Hippel (1974) and by Schwarz (1976). McGhee & von Hippel (1974) have derived an equation that expresses the free tropomyosin–troponin concentration, L_a or L_b, in terms of the binding density ν_a or ν_b and the binding constants K_a, and J_{aa} or K_b, and J_{bb}, respectively:

$$L_a = \left(\frac{1}{K_a}\right)\left(\frac{\nu_a}{1-7\nu_a}\right) \times \left[\frac{2(J_{aa}-1)(1-7\nu_a)}{(2J_{aa}+1)(1-7\nu_a)+\nu_a-R}\right]^6\left[\frac{2(1-7\nu_a)}{1-8\nu_a+R}\right]^2$$

where

$$R = [(1-8\nu_a)^2 + 4J_{aa}\nu_a(1-7\nu_a)]^{1/2} \quad (5)$$

L_a, ν_a, K_a, and J_{aa} can be replaced by L_b, ν_b, K_b, and J_{bb}.

The binding constants were fitted by seeking those pairs of constants for which the standard deviation of the calculated from the measured binding density reached a minimum. The results are summarized in Table I, and the calculated binding curves are displayed in Figure 6 as continuous lines. The deviations of the binding curves of tropomyosin–holotroponin measured in the presence of calcium from the calculated curve are within the range of experimental errors. Thus, the measured curve cannot be considered as significantly biphasic.

Table I: Equilibrium Constants for the Actin–Tropomyosin–Troponin Interaction

	equilibrium constant for binding to an isolated binding site (M^{-1})	equilibrium constant for moving of tropomyosin–troponin[a]
tropomyosin–holotroponin in the presence of calcium	6 600	250
tropomyosin–holotroponin in the absence of calcium	15 400	300
tropomyosin–troponin-T–I	17 500	200

[a] Moving from an isolated binding site to a singly contiguous binding site.

(*e*) *Binding Curves of Mixtures of Tropomyosin–Holotroponin and Tropomyosin–Troponin-T–I to Actin Filaments.* The samples contained four concentrations of tropomyosin–troponin-T–I (0.12, 0.24, 0.36, and 0.48 μM) and tropomyosin–holotroponin in the range 0.1–1.3 μM. The total actin concentration was kept constant at 7 μM. The binding curves were measured in the presence of calcium. A plot of the total tropomyosin–holotroponin concentration vs. the light-scattering intensity is depicted in Figure 7 for the four different concentrations of tropomyosin–troponin-T–I. In addition to the four known constants K_a, K_b, J_{aa}, and J_{bb}, the equilibrium of the assembly of the mixture of the two types of ligands with actin filaments is determined by the equilibrium constants J_{ab} and J_{ba} for the formation of the end-to-end contacts of different types of tropomyosin–troponin. These additional constants were fitted by seeking that set of binding curves that is in best agreement with the measured values. The binding curves were calculated as described under Appendix and Light Scattering. The criterion for the best agreement was that the standard deviation of the calculated from the measured normalized light-scattering intensity R_T/R_A reached a minimum. The best fit of equilibrium constants for formation of end-to-end contacts between tropomyosin–troponin in different positions on the actin filament was found to occur for $J_{ab} = J_{ba} = 115$. The calculated binding curves are depicted in Figure 7.

Good agreement was also reached when the ratio J_{ba}/J_{ab} was in the range from 0.1 to 1. In this range of ratios, the product of the fitted parameters J_{ba} and J_{ab} was nearly constant. In Figure 8, a plot of the ratio J_{ba}/J_{ab} vs. the product of J_{ab} and J_{ba} divided by the known values of J_{aa} and J_{bb} is shown. Below the ratio 0.1, the fit is poor. The calculated binding curves that represent the best fit for the ratio $J_{ba}/J_{ab} = 0$ ($J_{ba} = 0$, $J_{ab} = 960$) are displayed in Figure 9. Generation of a sequence of tropomyosin–troponin units in a different position on actin filaments appears to be 4-fold less favored than elongation of an existing sequence ($\sigma = {}^1/_4$).

(*f*) *Significance of the Binding Constants.* When only one type of ligand binds to actin filaments, the concentration of free ligand at half-saturation of actin filaments is nearly equal to the reciprocal of the equilibrium constant for binding of a ligand to a singly contiguous site (K_aJ_{aa} or K_bJ_{bb}). Since the free concentration of tropomyosin–troponin at half-saturation can be determined accurately (Figure 6), the products $K_aJ_{aa} = 1.65 \times 10^6$ M^{-1} and $K_bJ_{bb} = 3.5 \times 10^6$ are reliable values. If the end-to-end binding constants are high compared to the number of subunits covered by a ligand (J_{aa}, $J_{bb} \gg 7$), the

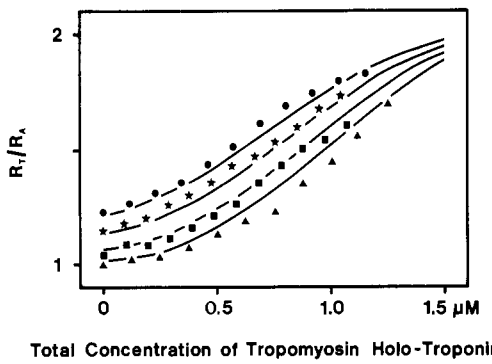

FIGURE 7: Normalized light-scattering intensities of mixtures of tropomyosin–holotroponin and tropomyosin–troponin-T–I (in the presence of calcium, 42.4 °C). Tropomyosin–troponin-T–I concentrations: (▲) 0.12 μM; (■) 0.24 μM; (☆) 0.36 μM; (●) 0.48 μM. The continuous lines represent the best fit ($J_{ab} = J_{ba} = 115$). The ratio R_T/R_A exceeds 1 at 0 concentration of tropomyosin–holotroponin because tropomyosin–troponin-T–I is present in one of the four concentrations.

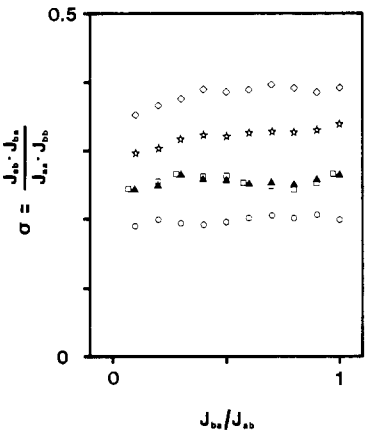

FIGURE 8: The cooperativity parameter σ calculated for different ratios of J_{ba} and J_{ab}. The equilibrium constants K_a, K_b, J_{aa}, and J_{bb} were varied in order to test the significance of the determined σ. (◇) K_a = 12 500 M^{-1}, J_{aa} = 125, K_b = 33 600 M^{-1}, and J_{bb} = 100; (☆) K_a = 12 500 M^{-1}, J_{aa} = 125, K_b = 8800 M^{-1}, and J_{bb} = 400; (▲) K_a = 6600 M^{-1}, J_{aa} = 250, K_b = 17 500 M^{-1}, and J_{bb} = 200; (□) K_a = 3400 M^{-1}, J_{aa} = 500, K_b = 33 600 M^{-1}, and J_{bb} = 100; (○) K_a = 3400 M^{-1}, J_{aa} = 500, K_b = 8800 M^{-1}, and J_{bb} = 400.

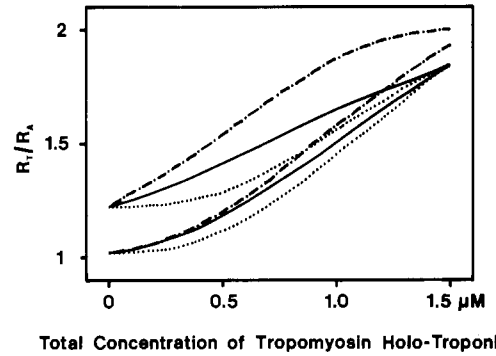

FIGURE 9: Binding curves calculated for different sets of equilibrium constants J_{ab} and J_{ba}. K_a = 6600 M^{-1}, J_{aa} = 250, K_b = 17 500 M^{-1}, and J_{bb} = 200. (- - -) $J_{ab} = J_{ba} = (J_{aa}J_{bb})^{1/2} = 223$, $\sigma = 1$; (···) $J_{ab} = J_{ba} = 0$, $\sigma = 0$; (—) $J_{ab} = 960$, $J_{ba} = 0$, $\sigma = 0$. Tropomyosin–troponin-T–I concentrations: lower curves, 0.12 μM; upper curves, 0.48 μM.

shape of the binding curves is not very sensitive to changes in the parameters J_{aa} and J_{bb} see McGhee & von Hippel (1974), Figure 7). Thus the determination of the values of K_a and J_{aa} or K_b and J_{bb} man not be as accurate as the determination of the product K_aJ_{aa} or K_bJ_{bb}.

In order to judge the significance of the found value of σ, it is necessary to consider the influence of errors in the determination of J_{aa} and J_{bb}. Therefore the cooperativity parameter σ was computed for pairs of K_a and J_{aa} or K_b and J_{bb} which differ from the determined values by a factor of about 2. Again it was found that the computed cooperativity parameters σ are quite independent of the ratio J_{ba}/J_{ab} and that the best agreement was reached when J_{ab} and J_{ba} were equal (Figure 8). Errors in the determination of J_{aa} or J_{bb} have a small influence on the fitted value of σ (Figure 8).

On the other hand, the shape of the binding curves depends strongly on the value of the cooperativity parameter σ, as can be seen from Figure 9 where binding curves for a random distribution of tropomyosin–troponin between the two positions on the actin filament ($\sigma = 1$) and for infinite cooperativity ($\sigma = 0$) are depicted. It appears that the cooperativity of a conformational change can be monitored quite significantly by the equilibrium analysis of the binding of two types of ligands to a filament.

Conclusions

The calcium-dependent shifting of tropomyosin–troponin on actin filaments has a small effect on the interaction of the tropomyosin–troponin complex with actin filaments. The affinities of tropomyosin–troponin for the two positions on actin filaments differ only by 2.6 kJ M^{-1} [$RT \ln (K_b/K_a)$ = 2.6 kJ M^{-1}]. The stronger binding in the absence of calcium is in agreement with studies by electron microscopy, showing that the contact of tropomyosin–troponin with actin filaments is closer in the absence than in the presence of calcium (Wakabayashi et al., 1975).

Generation of a sequence of tropomyosin–troponin units in a different position on actin filaments was found to be 4-fold less favored than elongation of an existing sequence ($\sigma = {}^1/_4$). Under conditions where as many tropomyosin–troponin units are situated in the groove as on the periphery of actin filaments, the average number of tropomyosin–troponin units adjacently situated in the same position is three (Applequist, 1963; eq 32). Thin filaments in muscle are composed of about 25 tropomyosin–troponin units. It appears that the shifting of tropomyosin–troponin on actin filaments is not an all-or-none reaction.

The difference in the binding affinities of tropomyosin–troponin for binding sites with an adjacent unit in the same or in a different position on an actin filament is only 2 kJ M^{-1} [$RT \ln (J_{aa}/J_{ab}) \approx RT \ln (J_{bb}/J_{ba}) \approx 2$ kJ M^{-1}]. This suggests that tropomyosin–troponin is so flexible that it can bend easily between the different positions on actin filaments. Certain segments of tropomyosin have been shown to be more readily cleaved by proteolytic enzymes than others (Pato & Smillie, 1978). This finding has been explained by variations in the stability of the coiled coil structure of tropomyosin. Also the disorder of tropomyosin crystals demonstrates the flexibility of this molecule (Cohen et al., 1971).

Binding of myosin to actin–tropomyosin–troponin filaments has been reported to increase the affinity of troponin for calcium (Bremel & Weber, 1972). Furthermore, attachment of myosin heads to actin filaments has been found to induce tropomyosin binding (Eaton, 1976). These two observations demonstrate that the properties of the tropomyosin–troponin system are changed by myosin binding to actin filaments. It is therefore an interesting question whether the cooperativity of the tropomyosin–troponin system is also modulated by the interaction of myosin with actin filaments.

Table II: Mass Action Equations for the Different Kinds of Binding Sites

no. (Figure 1)	kind of binding site or bound ligand	average no. per lattice of bound ligands	average no. per lattice of free binding sites: symbol	average no. per lattice of free binding sites: in terms of conditional probabilities	mass action equation
			Type a		
1	isolated	$A_{\text{-}}$	$U_{\text{-}}$	$U_{\text{-}} = (Aa_{\text{-}}f + Bb_{\text{-}}f)\left(\frac{ff^{s}}{1-ff}\right)$	$K_a = \frac{A_{\text{-}}}{L_a U_{\text{-}}}$
3	one adjacent ligand, a (left or right)	$A_{\text{-a-}}$	$U_{\text{-a-}}$	$U_{\text{-a-}} = (Aa_{\text{-}}f(2fa_1 + fb_1) + Bb_{\text{-}}f{\cdot}fa_1)\left(\frac{ff'}{1-ff}\right)$	$K_a J_{aa} = \frac{A_{\text{-a-}}}{L_a U_{\text{-a-}}}$
4	one adjacent ligand, b (left)	$A_{\text{b-}}$	$U_{\text{b-}}$	$U_{\text{b-}} = Bb_{\text{-}}f{\cdot}ff'$	$K_a J_{ba} = \frac{A_{\text{b-}}}{L_a U_{\text{b-}}}$
5	one adjacent ligand, b (right)	$A_{\text{-b}}$	$U_{\text{-b}}$	$U_{\text{-b}} = (Aa_{\text{-}}f + Bb_{\text{-}}f)fb_1\left(\frac{ff'}{1-ff}\right)$	$K_a J_{ab} = \frac{A_{\text{-b}}}{L_a U_{\text{-b}}}$
9	two adjacent ligands, a	$A_{\text{a-a}}$	$U_{\text{a-a}}$	$U_{\text{a-a}} = Aa_{\text{-}}f{\cdot}ff^{s}{\cdot}fa_1$	$K_a J_{aa}^{2} = \frac{A_{\text{a-a}}}{L_a U_{\text{a-a}}}$
10	two adjacent ligands, a (left), b (right)	$A_{\text{a-b}}$	$U_{\text{a-b}}$	$U_{\text{a-b}} = Aa_{\text{-}}f{\cdot}ff^{s}{\cdot}fb_1$	$K_a J_{aa} J_{ab} = \frac{A_{\text{a-b}}}{L_a U_{\text{a-b}}}$
11	two adjacent ligands, b (left), a (right)	$A_{\text{b-a}}$	$U_{\text{b-a}}$	$U_{\text{b-a}} = Bb_{\text{-}}f{\cdot}ff^{s}{\cdot}fa_1$	$K_a J_{ba} J_{aa} = \frac{A_{\text{b-a}}}{L_a U_{\text{b-a}}}$
12	two adjacent ligands, b	$A_{\text{b-b}}$	$U_{\text{b-b}}$	$U_{\text{b-b}} = Bb_{\text{-}}f{\cdot}ff^{s}{\cdot}fb_1$	$K_a J_{ba} J_{ab} = \frac{A_{\text{b-b}}}{L_a U_{\text{b-b}}}$
			Type b		
2	isolated	$B_{\text{-}}$	$V_{\text{-}}$	$V_{\text{-}} = (Aa_{\text{-}}f + Bb_{\text{-}}f)\left(\frac{ff^{s}}{1-ff}\right)$	$K_b = \frac{B_{\text{-}}}{L_b V_{\text{-}}}$
6	one adjacent ligand, b (left or right)	$B_{\text{-b-}}$	$V_{\text{-b-}}$	$V_{\text{-b-}} = (Bb_{\text{-}}f(2fb_1 + fa_1) + Aa_{\text{-}}f{\cdot}fb_1)\left(\frac{ff'}{1-ff}\right)$	$K_b J_{bb} = \frac{B_{\text{-b-}}}{L_b V_{\text{-b-}}}$
7	one adjacent ligand, a (left)	$B_{\text{a-}}$	$V_{\text{a-}}$	$V_{\text{a-}} = Aa_{\text{-}}f{\cdot}ff'$	$K_b J_{ab} = \frac{B_{\text{a-}}}{L_b V_{\text{a-}}}$
8	one adjacent ligand, a (right)	$B_{\text{-a}}$	$V_{\text{-a}}$	$V_{\text{-a}} = (Aa_{\text{-}}f + Bb_{\text{-}}f)fa_1\left(\frac{ff'}{1-ff}\right)$	$K_b J_{ba} = \frac{B_{\text{-a}}}{L_b V_{\text{-a}}}$
13	two adjacent ligands, b	$B_{\text{b-b}}$	$V_{\text{b-b}}$	$V_{\text{b-b}} = Bb_{\text{-}}f{\cdot}ff^{s}{\cdot}fb_1$	$K_b J_{bb}^{2} = \frac{B_{\text{b-b}}}{L_b V_{\text{b-b}}}$
14	two adjacent ligands, b (left), a (right)	$B_{\text{b-a}}$	$V_{\text{b-a}}$	$V_{\text{b-a}} = Bb_{\text{-}}f{\cdot}ff^{s}{\cdot}fa_1$	$K_b J_{bb} J_{ba} = \frac{B_{\text{b-a}}}{L_b V_{\text{b-a}}}$
15	two adjacent ligands, a (left), b (right)	$B_{\text{a-b}}$	$V_{\text{a-b}}$	$V_{\text{a-b}} = Aa_{\text{-}}f{\cdot}ff^{s}{\cdot}fb_1$	$K_b J_{ab} J_{bb} = \frac{B_{\text{a-b}}}{L_b V_{\text{a-b}}}$
16	two adjacent ligands, a	$B_{\text{a-a}}$	$V_{\text{a-a}}$	$V_{\text{a-a}} = Aa_{\text{-}}f{\cdot}ff^{s}{\cdot}fa_1$	$K_b J_{ab} J_{ba} = \frac{B_{\text{a-a}}}{L_b V_{\text{a-a}}}$

Appendix

Equilibrium of the Association of Two Types of Large Ligands with a One-Dimensional Homogeneous Lattice. The approach for deriving binding equations follows the treatment introduced by McGhee & von Hippel (1974) for their model of cooperative binding of large ligands to a one-dimensional homogeneous lattice. The approach presented in this section is essentially an extension of this model to a mixture of two types of ligands.

Mass Action Equations. We consider linear lattices consisting of N subunits. N is assumed to be so large that end effects can be neglected. This means that the average length of gaps or of ligand clusters along the lattice is small compared to N. Under a particular set of experimental conditions, an average number A or B of ligands of type a or b, respectively, are bound to a lattice. The average number of bound ligands of type a or b per lattice subunit (binding density) is given by $\nu_a = A/N$ or $\nu_b = B/N$, respectively. For both types of ligands, eight kinds of binding sites that differ in the binding constants (Figure 1) are conceivable. Correspondingly one can subdivide the average numbers A and B of bound ligands into the average numbers of ligands bound to each of the eight kinds of binding sites. In Table II the symbols as well as the definitions for the average numbers are listed. In order to formulate mass action equations, one has furthermore to introduce the average numbers per lattice of all kinds of binding sites and the free concentrations L_a and L_b of the two types of ligands a and b, respectively (see Table II).

In many cases, it is not possible to measure the concentrations of the individual kinds of bound ligands or free binding sites. Usually colligative properties such as free concentrations (L_a and L_b) or binding densities (ν_a and ν_b) can be determined experimentally. Conditional probabilities will be introduced in the next section in order to express the concentrations of the different kinds of bound ligands and free binding sites in terms of binding constants, binding densities, and free concentrations.

Conditional Probabilities. We designate the subunits of the lattice corresponding to the bound ligand. Subunits that are covered by a ligand of type a or b are labeled a or b, respectively. A free subunit is labeled with f. The ligands can

be divided into seven sections, each of which covers one subunit of the lattice. The sections are numbered from left to right. A subunit under section number n is labeled a_n or b_n, respectively (Figure 10). We adopt the convention that the subunits are considered from left to right. Thus, the conditional probability is defined by the probability, given a subunit in state a_n, b_n, or f, that the subunit immediately on the right is present in state a_m, b_m, or f. The conditional probabilities are termed by the combination of the states of two adjacent subunits; e.g., fa_1 is the probability, given a subunit free of a ligand, that the subunit immediately on the right is covered by the left end of ligand a.

Of the 15^2 different conditional probabilities, only nine probabilities depend on the equilibrium constants and the concentrations of ligands. The values of the rest of the conditional probabilities are 1 or 0, depending on whether or not two states of a subunit can occur in adjacent positions [e.g., $a_n a_{n+1} = 1$ $(n < 7)$ and $a_n a_{n+2} = 0$ $(n < 6)$]. The nine conditional probabilities of interest are displayed in Figure 10. For the calculation of the nine conditional probabilities, nine equations are necessary. Three equations stem from the consideration that the subunit adjacent on the immediate right of another subunit in the state a_7, b_7, is either a_1, b_1, or f. Hence:

$$a_7a_1 + a_7b_1 + a_7f = 1 \tag{6a}$$

$$b_7a_1 + b_7b_1 + b_7f = 1 \tag{6b}$$

$$fa_1 + fb_1 + ff = 1 \tag{6c}$$

Moreover, the conditional probabilities can be related to the ligand–ligand interaction equilibrium constants J_{aa}, J_{ab}, J_{ba}, and J_{bb}. The equations may be obtained with the aid of Figure 11. The two ligand configurations depicted in Figure 11 differ in that the right ligand is moved from an isolated binding site in the first configuration to a singly contiguous binding site in the second configuration. Since J_{aa} is the equilibrium constant for the reaction displayed in Figure 11, the ratio of the probabilities of the two configurations is equal to J_{aa}.

$$J_{aa} = \frac{fa_1 \cdot a_7a_1 \cdot a_7f \cdot ff^5}{fa_1 \cdot a_7f \cdot ff^4 \cdot fa_1 \cdot a_7f} = \frac{a_7a_1 \cdot ff}{a_7f \cdot fa_1} \tag{6d}$$

In analogy one can derive equations for J_{ab}, J_{ba}, and J_{bb}.

$$J_{ab} = \frac{a_7b_1 \cdot ff}{a_7f \cdot fb_1} \tag{6e}$$

$$J_{ba} = \frac{b_7a_1 \cdot ff}{b_7f \cdot fa_1} \tag{6f}$$

$$J_{bb} = \frac{b_7b_1 \cdot ff}{b_7f \cdot fb_1} \tag{6g}$$

Two additional equations result from the consideration that the probability of a subunit selected at random being the left end of a ligand of type a is equal to ν_a. The subunit to the left of the selected subunit either is covered by the right end of a ligand of type a or b or is free. The probability of the subunit to the left being covered by the right end of a ligand of type a or b is ν_a or ν_b, respectively, and the probability of the subunit to the left being free is equal to $\varphi = 7\nu_a - 7\nu_b$. Hence:

$$\nu_a \cdot a_n a_1 + \nu_b \cdot b_n a_1 + \varphi \cdot fa_1 = \nu_a \tag{6h}$$

The probability of a subunit selected at random being free is equal to φ. The subunit to the left is either free (probability φ) or covered by the right end of a ligand of type a or b (probabilities ν_a or ν_b, respectively). Hence:

$$\nu_a \cdot a_n f + \nu_b \cdot b_n f + \varphi \cdot ff = \varphi \tag{6i}$$

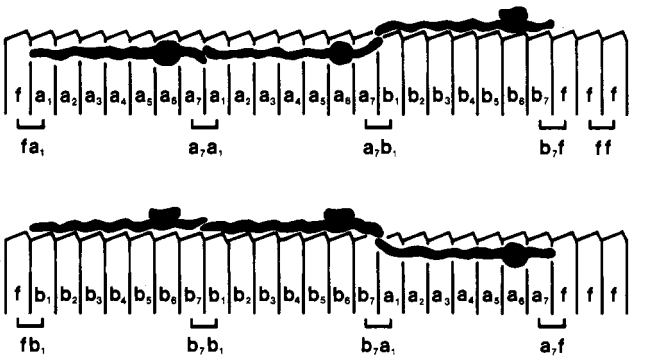

FIGURE 10: Labeling of actin filament subunits corresponding to the bound ligand. The conditional probabilities are displayed as combinations of two labels of actin subunits.

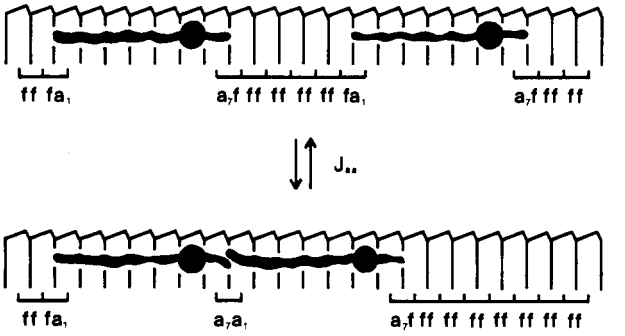

FIGURE 11: Reaction scheme for moving the right ligand from an isolated binding site to a singly contiguous binding site. The ratio of the probabilities of the two configurations is J_{aa}.

When eq 6a–i are used, the nine conditional probabilities can be calculated for a set of equilibrium constants J_{aa}, J_{ab}, J_{ba}, and J_{bb} and of binding densities ν_a, ν_b, and φ.

Mass Action Equations in Terms of Equilibrium Constants, Binding Densities, and Free Concentrations of Ligands. The length distribution of gaps under a set of equilibrium constants, binding densities, and free ligand concentrations can be constructed by means of conditional probabilities. The length distribution may be described by the probability that a gap terminated by a ligand of type a or b on the left is g lattice subunits long and that the residue at the right terminus of the gap is of type a or b. P_{agb} is defined as the probability that a gap terminated by a ligand of type a on the left is g lattice subunits long and that the ligand at the right terminus is of type b. P_{aga}, P_{bga}, and P_{bgb} are defined in analogy. The probability P_{a2b} that a gap with a ligand of type a at the left terminus is two lattice subunits long and that the gap is terminated by a ligand of type b on the right can be expressed by conditional probabilities thus: P_{a2b} = (the probability, having selected the right end of a bound ligand of type a, that the lattice subunit to the right is free) × (the probability, given a free residue, that the lattice residue to the right is free, too) × (the probability, given a free residue, that the left end of a ligand of type b covers the lattice subunit to the right) = $a_7f \cdot ff \cdot fb_1$. Generally the probabilities P_{aga}, P_{agb}, P_{bga}, and P_{bgb} are given by

$$P_{aga} = a_7f \cdot ff^{g-1} \cdot fa_1 \tag{7a}$$

$$P_{agb} = a_7f \cdot ff^{g-1} \cdot fb_1 \tag{7b}$$

$$P_{bga} = b_7f \cdot ff^{g-1} \cdot fa_1 \tag{7c}$$

$$P_{bgb} = b_7f \cdot ff^{g-1} \cdot fb_1 \tag{7d}$$

The number of isolated binding sites per gap being g lattice subunits long is $g - 8$. The average number i_a of isolated binding sites per gap with a ligand of type a at the left terminus

and a ligand of type a or b at the right terminus is obtained by summing up the number of binding sites multiplied by the probability $P_{aga} + P_{agb}$ that a gap has the length to contain this number of binding sites.

$$i_a = \sum_{g=9}^{\infty} [(g-8)(P_{aga} + P_{agb})] = a_7 f(fa_1 + fb_1) \sum_{g=9} [(g-8) ff^{g-1}] = a_7 f\left(\frac{ff^8}{1-ff}\right) \quad (8a)$$

Correspondingly the average numbr i_b of isolated binding sites per gap with a ligand of type b at the left terminus and a ligand of type a or b at the right terminus is obtained.

$$i_b = \sum_{g=9}^{\infty} [(g-8)(P_{bga} + P_{bgb})] = b_7 f\left(\frac{ff^8}{1-ff}\right) \quad (8b)$$

The average number per lattice of gaps with a ligand of type a or b at the left terminus is equal to the number A or B of bound ligands of type a or b, respectively (counting the gap length from $g = 0$). Hence, the average number U_- of isolated binding sites per lattice is given by

$$U_- = Ai_a + Bi_b = (Aa_7 f + Bb_7 f)\left(\frac{ff^8}{1-ff}\right) \quad (9)$$

The average numbers per lattice of the other kinds of binding sites can be obtained by following the same procedure and are listed in Table II. Summing the mass action equations derived for all kinds of bound ligands of type a or b, we arrive at overall binding equations:

$$K_a L_a \left\{ (\nu_a a_7 f + \nu_b b_7 f)\left(\frac{ff^8}{1-ff}\right) + J_{aa}[\nu_a a_7 f(2fa_1 + fb_1) + \nu_b b_7 ffa_1]\left(\frac{ff^7}{1-ff}\right) + J_{ab}(\nu_a a_7 f + \nu_b b_7 f) fb_1 \left(\frac{ff^7}{1-ff}\right) + J_{ba}\nu_b b_7 f \cdot ff^7 + (J_{aa}\nu_a a_7 f + J_{ba}\nu_b b_7 f)(J_{aa} fa_1 + J_{ab} fb_1) ff^6 \right\} = \nu_a \quad (10a)$$

and

$$K_b L_b \left\{ (\nu_a a_7 f + \nu_b b_7 f)\left(\frac{ff^8}{1-ff}\right) + J_{bb}[\nu_b b_7 f(2fb_1 + fa_1) + \nu_a a_7 f \cdot fb_1]\left(\frac{ff^7}{1-ff}\right) + J_{ba}(\nu_a a_7 f + \nu_b b_7 f) fa_1 \left(\frac{ff^7}{1-ff}\right) + J_{ab}\nu_a a_7 f \cdot ff^7 + (J_{bb}\nu_b b_7 f + J_{ab}\nu_a a_7 f)(J_{bb} fb_1 + J_{ba} fa_1) ff^6 \right\} = \nu_b \quad (10b)$$

In these binding equations, the sum of all kinds of bound ligands was replaced by the average number of bound ligands per lattice, $A = \nu_a N$ and $B = \nu_b N$.

Acknowledgments

We thank Dr. Annemarie Weber for discussions.

References

Applequist, J. (1963) *J. Chem. Phys.* **38**, 934–941.
Bremel, R. D., & Weber, A. (1972) *Nature (London), New Biol.* **238**, 97–101.
Casassa, E. F. (1955) *J. Chem. Phys.* **23**, 596–597.
Clarke, F. M., Lovell, S. J., Masters, C. J., & Winzor, D. J. (1976) *Biochim. Biophys. Acta* **427**, 617–626.
Cohen, C., Caspar, D. L. D., Parry, D. A. D., & Lucas, R. M. (1971) *Cold Spring Harbor Symp. Quant. Biol.* **36**, 205–216.
Collins, J. H., Greaser, M. L., Potter, J. D., & Horn, M. J. (1977) *J. Biol. Chem.* **252**, 6356–6362.
Eaton, B. L. (1976) *Science (Washington, D.C.)* **192**, 1337–1339.
Ebashi, S. (1963) *Nature (London)*, **200**, 1010.
Ebashi, S., Wakabayashi, T., & Ebashi, F. (1971) *J. Biochem. (Tokyo)* **69**, 441–445.
Eisenberg, E., & Kielley, W. W. (1974) *J. Biol. Chem.* **249**, 4742–4748.
Elzinga, M., Collins, J. H., Kuehl, W. M., & Adelstein, R. S. (1973) *Proc. Natl. Acad. Sci. U.S.A.* **70**, 2687–2691.
Greaser, M. L., & Gergely, J. (1971) *J. Biol. Chem.* **246**, 4226–4233.
Greaser, M. L., Yamaguchi, M., Brekke, C., Potter, J., & Gergely, J. (1972) *Cold Spring Harbor Symp. Quant. Biol.* **37**, 235–244.
Greene, L., & Eisenberg, E. (1980) *Proc. Natl. Acad. Sci. U.S.A.* **77**, 2616–2620.
Haselgrove, J. C. (1972) *Cold Spring Harbor Symp. Quant. Biol.* **37**, 341–352.
Hill, T. L., Eisenberg, E., & Greene, L. (1980) *Proc. Natl. Acad. Sci. U.S.A.* **77**, 3186–3190.
Horwitz, J., Bullard, B., & Mercola, D. (1979) *J. Biol. Chem.* **254**, 350–355.
Huxley, H. E. (1972) *Cold Spring Harbor Symp. Quant. Biol.* **37**, 361–376.
Ising, E. (1925) *Z. Phys.* **31**, 526.
Laemmli, U. K. (1970) *Nature (London)* **227**, 680–685.
Lehrer, S. S. (1975) *Proc. Natl. Acad. Sci. U.S.A.* **72**, 3377–3381.
Margossian, S. S., & Cohen, C. (1973) *J. Mol. Biol.* **81**, 409–413.
McGhee, J. D., & von Hippel, P. (1974) *J. Mol. Biol.* **86**, 469–489.
Oosawa, F., & Kasai, M. (1962) *J. Mol. Biol.* **4**, 10–21.
Parry, D. A. D., & Squire, J. M. (1973) *J. Mol. Biol.* **75**, 33–55.
Pato, M. D., & Smillie, L. B. (1978) *FEBS Lett.* **87**, 95–98.
Pearlestone, J. R., Carpenter, M. R., Johnson, P., & Smillie, L. B. (1976) *Proc. Natl. Acad. Sci. U.S.A.* **73**, 1902–1906.
Rees, M. K., & Young, M. (1967) *J. Biol. Chem.* **242**, 4449–4458.
Schwarz, G. (1976) *Biophys. Struct. Mech.* **2**, 1–12.
Seymour, J., & O'Brien, E. J. (1980) *Nature (London)* **283**, 680–682.
Sperling, J. E., Feldmann, K., Meyer, H., Jahnke, U., & Heilmeyer, L. M. G. (1979) *Eur. J. Biochem.* **101**, 581–592.
Spudich, J. A., & Watt, S. (1971) *J. Biol. Chem.* **246**, 4866–4871.
Stone, D., Sodek, J., Johnson, P., & Smillie, L. B. (1975) *Proc. FEBS Meet.* **31**, 125–136.
Wakabayashi, T., Huxley, H. E., Amos, L. A., & Klug, A. (1975) *J. Mol. Biol.* **93**, 477–497.
Walsh, T. P., & Wegner, A. (1980) *Biochim. Biophys. Acta* **626**, 79–87.
Wegner, A. (1976) *J. Mol. Biol.* **108**, 139–150.
Wegner, A. (1979) *J. Mol. Biol.* **131**, 839–853.
Wegner, A. (1980) *FEBS Lett.* **119**, 245–248.
Wegner, A., & Engel, J. (1975) *Biophys. Chem.* **3**, 215–225.
Wilkinson, J. M. (1974) *Biochim. Biophys. Acta* **359**, 379–388.
Wilkinson, J. M., & Grand R. J. A. (1975) *Biochem. J.* **149**, 493–496.
Zimm, B. H., & Bragg, J. K. (1959) *J. Chem. Phys.* **31**, 526–531.